47th AIAA Aerospace Sciences Meeting Including The New Horizons Forum and Aerospace Exposition
5 - 8 January 2009, Orlando, Florida

AIAA 2009-1429

Numerical Simulation of Temperature-Dependent, Anisotropic Tertiary Creep Damage

Calvin Stewart[1], Ali P. Gordon[2], and David W. Nicholson[3]
Department of Mechanical, Materials, and Aerospace Engineering, University of Central Florida, Orlando, FL 32816-2450

Directionally-solidified (DS) Ni-base superalloys are commonly applied as turbine materials to primarily withstand creep conditions manifested in either marine-, air- or land-based gas turbines components. The thrust for increased efficiency of these systems, however, translates into the need for these materials to exhibit considerable strength and temperature resistance. Accurate prediction of crack initiation behavior of these hot gas path components is an on-going challenge for turbine designers. Aside from the spectrum of mechanical loading, blades and vanes are subjected to high temperature cycling and thermal gradients. Imposing repeated start-up and shut-down steps leads to creep and fatigue damage. The presence of stress concentrations due to cooling holes, edges, and sites sustain foreign object damage must also be taken into account. These issues and the interaction thereof can be mitigated with the application of high fidelity constitutive models implemented to predict material response under given thermomechanical loading history. In the current study, the classical Kachanov-Rabotnov model for tertiary creep damage is implemented in a general-purpose finite element analysis (FEA) software. The evolution of damage is considered as a vector-valued quantity to account for orientation-dependent damage accumulation. Creep deformation and rupture experiments on samples from a representative DS Ni-base superalloys tested at temperatures between 649 and 982°C and three orientations (longitudinally-, transversely-oriented, and intermediately oriented). The damage model coefficients corresponding to secondary and tertiary creep constants are characterized for temperature and orientation dependence. This advanced formulation can be implemented for modeling full-scale parts containing temperature gradients.

Nomenclature

A,n	=	secondary creep constants
B,l,k	=	tertiary creep constants
$\mathbf{I}$	=	identity tensor
$\mathbf{n_1}$	=	first principal direction of the effective stress tensor
$\tilde{\mathbf{s}}$	=	deviatoric stress of the effective stress tensor
α,β	=	weighing factors in the Hayhurst stress
γ	=	isotropic/anisotropic control variable
$\boldsymbol{\varepsilon}$	=	strain tensor
$\boldsymbol{\sigma}$	=	stress tensor
$\tilde{\boldsymbol{\sigma}}$	=	effective stress tensor
σ_{Ω}^{eq}	=	Hayhurst (triaxial) stress of the effective stress tensor
$\tilde{\sigma}_1$	=	first principal stress of the effective stress tensor
$\tilde{\sigma}_H$	=	hydrostatic (mean) stress of the effective stress tensor
$\tilde{\sigma}_{VM}$	=	von Mises stress of the effective stress tensor
$\boldsymbol{\Phi}$	=	damage applied
ω	=	damage
$\boldsymbol{\Omega}$	=	damage tensor
$\dot{\boldsymbol{\Omega}}$	=	damage rate tensor

[1] Graduate Student, cmstewar@mail.ucf.edu, Member AIAA.
[2] Assistant Professor, apgordon@mail.ucf.edu, Member AIAA.
[3] Professor, nicholsn@mail.ucf.edu, Member AIAA.

I. Introduction

Creep is the inelastic deformation of a material due to high temperature. As temperature increases the creep strain rate increases accordingly. Early work in the field of creep continuum mechanics focused solely on modeling the isotropic creep strain rate. One such example is the Norton power law for secondary creep. Further development, geared towards including the non-linear strain experience in the tertiary creep regime caused the inclusion of the concept of damage. This is where the creep strain rate is influenced by the degraded or damage state of the material at each time step. It results in a damage evolution equation being coupled with the creep strain rate equation.

Isotropic creep models work best when the mechanical load experienced by a component is similar to what is applied during uniaxial creep tests. Such models are inappropriate for modeling components which undergo complex states of stress. In most cases, the off-axis components of a stress tensor in the vicinity of stress raisers, cracks, and notches have non-zero values and the stress state is more complex than that which can be achieved in conventional creep testing. Moreover, the dependence of creep rate is strongly non-linear with stress; therefore, creep damage may also depend on the 'direction' of the stress vector as well as on the absolute value of its components. Additionally, isotropic creep models are unable to model the orientation dependence of material properties. An isotropic-scalar compliance term cannot replicate anisotropic compliance tensor in symmetry classes such as triclinic, orthotropic, transversely isotropic materials, and so on.

Drives by the aerospace and power generation industries to increase turbine efficiency have produced a massive influx in the development of anisotropic alloys since the 1980's.[1] Through the process of directional solidification, material manufacturers can directly control the alignment of grain boundaries. Such alloys are design to produce enhanced strength, stiffness, and/or creep resistance in a particular orientation. When used on turbine blades, they are manufactured so that the enhanced material direction is aligned with the direction where the most mechanical load is experienced. This process produces gas turbine components which have longer lives.

Of particular importance to both aerospace and the power generation industries is the temperature gradient experienced by turbine components. In power generation, gas turbines experience cyclic thermomechanical loading occurs due to peak power requirements. Repeated startup and shutdown steps lead to creep and fatigue damage. In the aerospace industry the thermal gradient across the turbine changes as a function of flight history and maneuvers. These changes affect the rate at which creep occurs across the component. Both industries deal with thermal variations which necessitate a creep model which includes temperature-dependence.

An anisotropic tertiary creep damage model is implemented in the ANSYS finite element software. The creep material properties are optimized over a range of temperatures and material orientations. Through regression analysis, temperature-dependent and orientation-dependent functions are developed for each material property. Comparison between available creep deformation data and the simulations is conducted to verify the accuracy of the anisotropic tertiary creep damage material model.

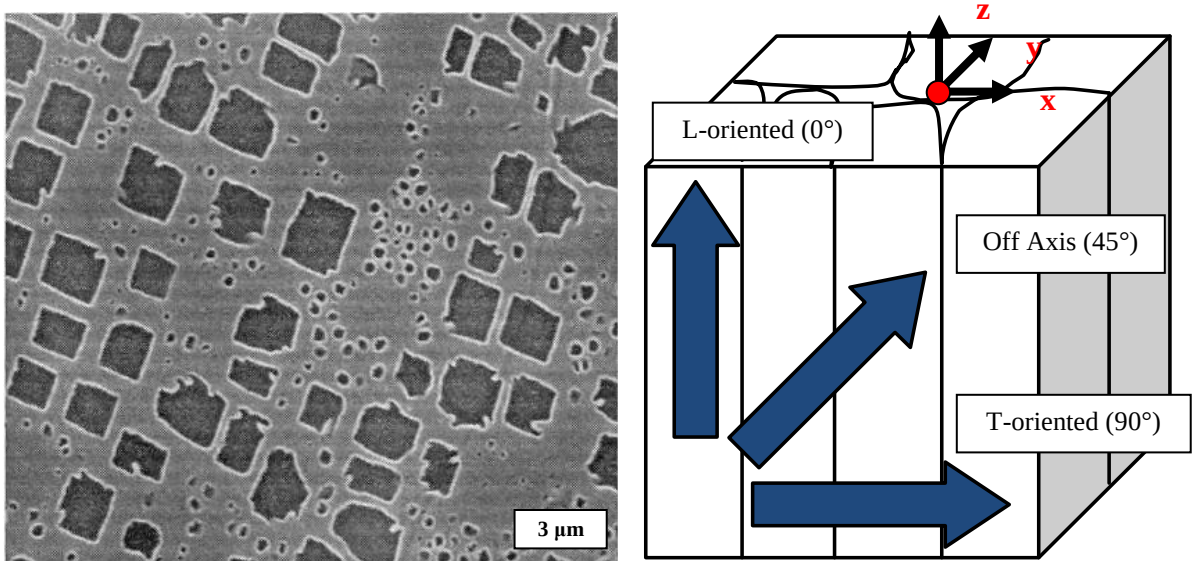

Figure 1. Structure of GTD-111 (a) Image of microstructure. Dark areas are the bimodal γ' precipitated particles (b) Schematic of grain structure

Table 1. Nominal chemical composition of GTD-111 superalloy[3]

Cr	Co	Al	Ti	W	Mo	Ta	C	Zr	B	Fe	Si	Mn	Cu	P	S	Ni
13.7	9.0	2.8	4.7	3.5	1.4	2.5	0.1	0.0	-	-	-	-	-	-	-	Bal.
14.3	10.0	3.2	5.1	4.1	1.7	3.1	0.1	0.0	0.0	0.4	0.3	0.1	0.1	0.0	0.0	Bal.

II. Material

The material under consideration is GTD-111, a directionally-solidified (DS) Ni-base superalloy commonly used in gas turbine blading. Directional solidification is a technique by which the grain structure of the material can be aligned in a particular orientation. This produces a material that has enhanced stiffness, strength, and creep rupture properties in one or more local coordinate directions.

Alloy DS GTD-111 was developed in the 1980's and is a modification of the GE superalloy Rene' 80.[2] It is a transversely isotropic material where solidification occurs in the <001> longitudinal (L) orientation while the transversely (T) orientations <100> and <010>, are uncontrolled. Microstructurally, GTD-111 is formed of a nickel austenite (γ) matrix, bimodal gamma prime (γ') precipitated particles, $\gamma - \gamma'$ eutectic, carbides and small amounts of topological close-packed phases σ, δ, η and laves.[3,4] The matrix and (γ') precipitated particles are observed in Fig. 1a. It has a high volume fraction of gamma prime (γ') precipitated particles, (>60%) which impart enhanced impact strength, high temperature creep and fatigue resistance, and improve corrosion resistance. This microstructure causes difficulties when considering component repair but a number of methods are under investigation to mitigate this problem. [2,5] The nominal chemical composition can be found in Table 1.

Due to the directionally solidified nature of the material, the creep strain rate is dependent on orientation. This is due to the grain structure being aligned in the <001> direction. Figure 1b depicts where grains are longitudinally (L) and transversely (T) oriented. Of particular interest is the creep response at off axis locations (such as 45°) where an intermediate response between L and T is expected to occur.

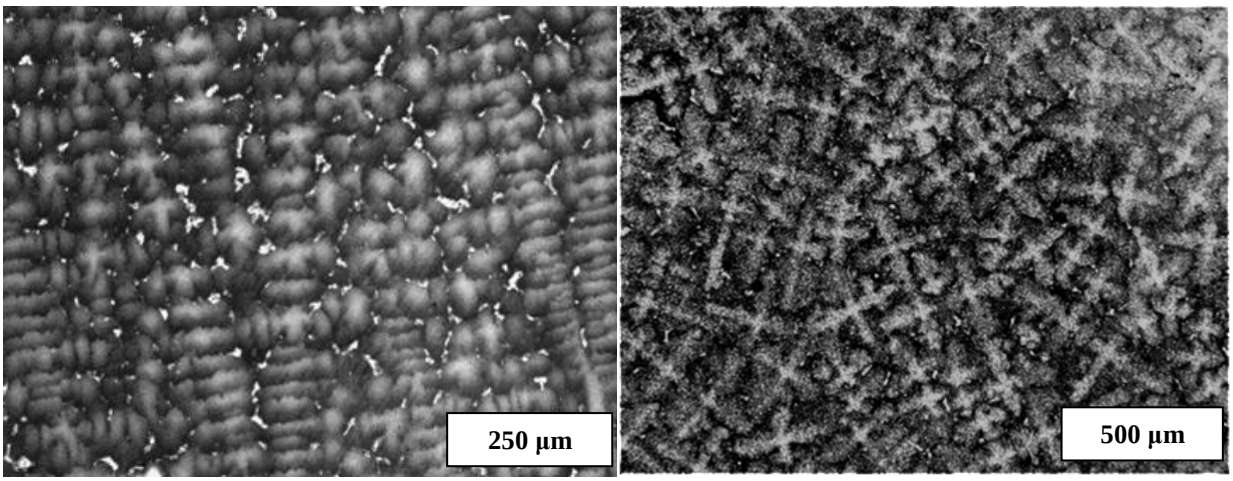

Figure 2. Grain structure of GTD-111 (a) T-oriented Specimen (b) L-oriented Specimen

Through optical and scanning electron microscopy investigations, a closer look at the grain structure of the material was resolved. Figure 2 shows the grain structure of both L and T-orientations. It shows that in the T-oriented directions long grain boundaries are found. In the L-oriented direction a textured pattern is observed. The material behavior in the transverse directions <100> and <010> is similar to that of polycrystalline (PC) materials.

Creep deformation and rupture tests were performed on L and T-oriented specimen. A parametric study including temperatures ranging from 649 to 982°C and varying stress levels was implemented to determine the creep response of the material over a wide range of conditions. Figure 3 demonstrates the creep response at 871°C. This collected data was used to compare the experimental results with those that are numerically simulated.

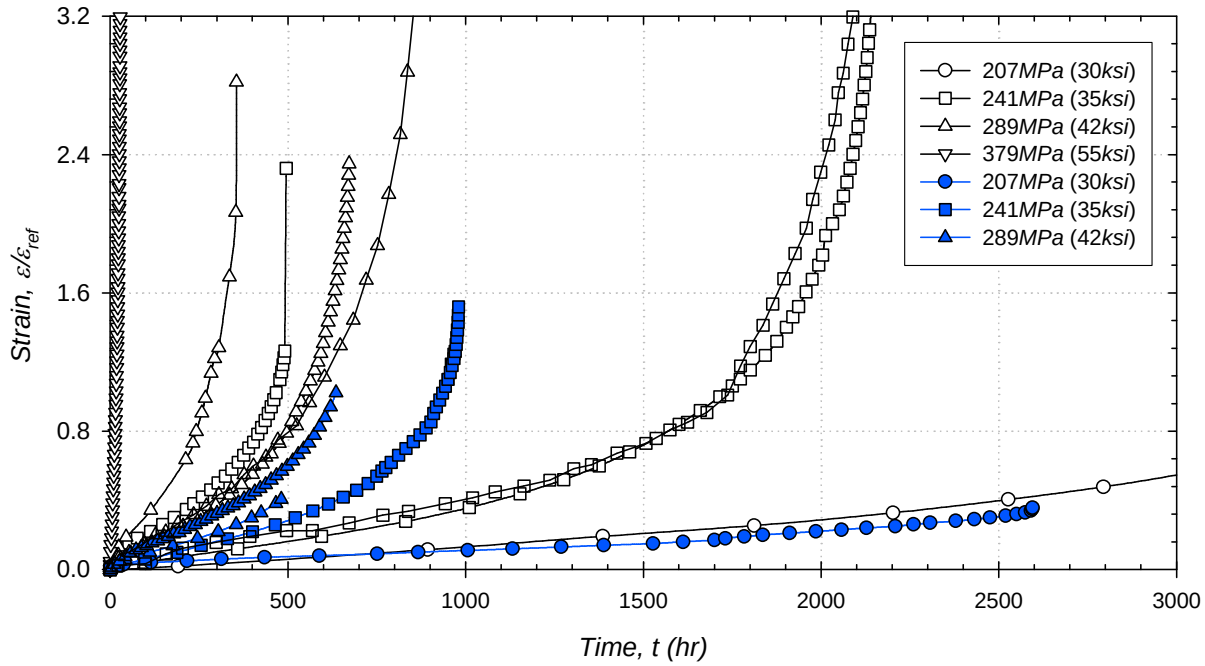

Figure 3. Creep deformation of L-oriented (unfilled symbols) and T-oriented (filled symbols) GTD-111 superalloy at 871°C.

III. Anisotropic Creep Damage Model

Modern creep continuum damage models are based off two fundamental equations, creep rate and damage evolution. Early work in the field consisted solely of the isotropic creep rate, such as the Norton power law for secondary creep. These models are limited because they do not include the non-linear enhanced creep deformation during the tertiary creep stage. More advanced isotropic models included damage evolution which relates the net reduction in area of a material as it deforms to the applied stress.[6] These models are powerful but assume that damage is scalar and isotropic when it is not. Literature has shown that damage is fundamentally anisotropic.[7,8] Due to inconsistencies during material processing, specimen do not have completely uniform, homogenous, grain structures and therefore upon loading experience anisotropic damage. This damage causes the inelastic deformation of the material to differ dependent upon local orientation. Tensor based, anisotropic tertiary creep damage models are therefore requirement.

The anisotropic creep damage model used to fulfill this requirement is fundamentally based off the isotropic Kachanov[9]-Rabotnov[10] creep damage model with the application of the Hayhurst (triaxial) stress.[11] The anisotropic tensor based formulation starts with the effective stress tensor, $\tilde{\boldsymbol{\sigma}}$. Murakami[12] and Murakami and Ohno[13] proposed the tensor based, anisotropic extension of the effective stress and damage applied as

$$\tilde{\boldsymbol{\sigma}} = \frac{1}{2}\left(\boldsymbol{\sigma}\cdot\boldsymbol{\Phi} + \boldsymbol{\Phi}\cdot\boldsymbol{\sigma}\right)$$
$$\boldsymbol{\Phi} = \left(\mathbf{I} - \boldsymbol{\Omega}\right)^{-1} \tag{1}$$

where $\boldsymbol{\sigma}$ is the applied stress tensor and $\boldsymbol{\Omega}$ is the secondary rank damage tensor. Damage is thus considered the three-dimensional degradation of the material due to voids and fissure growth in the material over time. Hayhurst[14] determined from creep rupture tests that for a number of creep resistant alloys, void and fissure growth on grain boundaries occurs at planes 90° perpendicular to the principal stress direction, where a majority of damage is concentrated on the plane perpendicular (0°) to the first principal stress, $\tilde{\sigma}_1$. Using the terms of the effective stress tensor, the Hayhurst (triaxial) stress is applied relating the first principal stress, $\tilde{\sigma}_1$, hydrostatic (mean) stress, $\tilde{\sigma}_H$, and von Mises stress, $\tilde{\sigma}_{VM}$.[11] The Hayhurst stress is given as

$$\sigma_{\Omega}^{eq} = \alpha\tilde{\sigma}_1 + 3\beta\tilde{\sigma}_H + (1-\alpha-\beta)\tilde{\sigma}_{VM} \tag{2}$$

where α and β are weighing factors valued between zero and one and are determined from multiaxial creep experiments. The damage evolution equation is given as

$$\dot{\boldsymbol{\Omega}} = B\left(\left\langle\sigma_{\Omega}^{eq}\right\rangle\right)^{l}\left[tr\left(\boldsymbol{\Phi}\cdot\mathbf{n_1}\otimes\mathbf{n_1}\right)\right]^{k-l}\left[(1-\gamma)\mathbf{I}+\gamma\mathbf{n_1}\otimes\mathbf{n_1}\right] \tag{3}$$

where $\mathbf{n_1}$ is the first principle direction vector and *B*, *k*, *l*, and γ are tertiary creep constants. An attractive property of this anisotropic tertiary creep damage model is the inherit ability to revert to the isotropic Kachanov-Rabotnov tertiary creep damage model. When γ is equal to zero, the damage evolution equation will revert to a scalar form (i.e. an isotropic form). Conversely, increasing γ results in enhanced material degradation on planes perpendicular to the principal direction $\mathbf{n_1}$ (γ = 1.0 is considered fully anisotropic). Taking the previous terms and applying them in the Norton power law results in the following creep rate equation,

$$\dot{\boldsymbol{\varepsilon}}^{cr} = \frac{3}{2}A\left(\tilde{\sigma}_{VM}\right)^{n}\frac{\tilde{\mathbf{s}}}{\tilde{\sigma}_{VM}} \tag{4}$$

where $\tilde{\mathbf{s}}$ is the deviatoric stress tensor and *A* and *n* are secondary creep material constants. Using Eqs. (3) and (4), the creep deformation response of an anisotropic material can be modeled.

IV. Numerical Methodology

The anisotropic tertiary creep damage model has been implemented into the finite element analysis (FEA) software ANSYS. This was achieved by coding a user-programmable feature (UPF) material model subroutine in FORTRAN. This subroutine incorporates the backward Euler implicit-integration algorithm which allows long time simulations to be conducted with limited error. The material model was written into the USERMAT UPF.

The USERMAT UPF allows the user to establish a unique total (reduced) stiffness tensor. This was done as follows

$$\begin{aligned}\boldsymbol{\varepsilon} &= \mathbf{S}_{EL}\cdot\boldsymbol{\sigma} + \mathbf{S}_{INEL}\cdot\boldsymbol{\sigma}\\ \mathbf{Q}_{TOT} &= \left(\mathbf{S}_{EL}\right)^{-1} + \left(\mathbf{S}_{INEL}\right)^{-1}\end{aligned} \tag{5}$$

where $\boldsymbol{\varepsilon}$ is the total strain tensor, $\boldsymbol{\sigma}$ is the stress tensor, $\mathbf{S}_{\mathrm{EL}}$ is the elastic compliance tensor, $\mathbf{S}_{\mathrm{INEL}}$ is the creep (inelastic) compliance tensor, and $\mathbf{Q}_{\mathrm{TOT}}$ is the total (reduced) stiffness tensor. Considering that GTD-111 is a transversely isotropic material, a total of six material properties are necessary to determine the elastic compliance tensor, $\mathbf{S}_{\mathrm{EL}}$. The elastic compliance tensor then takes the following form.

$$\mathbf{S}_{EL} = \begin{bmatrix} \frac{1}{E_p} & -\frac{\nu_p}{E_p} & -\frac{\nu_{zp}}{E_z} & 0 & 0 & 0 \\ -\frac{\nu_p}{E_p} & \frac{1}{E_p} & -\frac{\nu_{zp}}{E_z} & 0 & 0 & 0 \\ -\frac{\nu_{pz}}{E_p} & -\frac{\nu_{pz}}{E_p} & \frac{1}{E_z} & 0 & 0 & 0 \\ 0 & 0 & 0 & \frac{1}{G_{zp}} & 0 & 0 \\ 0 & 0 & 0 & 0 & \frac{1}{G_{zp}} & 0 \\ 0 & 0 & 0 & 0 & 0 & 2\left(\frac{1+\nu_p}{E_p}\right) \end{bmatrix} \tag{6}$$

The Young's modulus and Poisson's ratio on the <100> and <010> oriented x-y symmetry plane are defined as E_p and ν_p respectively. The <001> z-oriented Young's modulus, Poisson's ratios, and Shear modulus are defined as E_z, ν_{zp}, ν_{pz}, and G_{zp}, respectively. The creep (inelastic) compliance tensor, $\mathbf{S}_{INEL}$, was derived using the creep strain rate Eq. (4) and effective stress tensor Eq. (1) into the following triclinic symmetric form.

$$\mathbf{S}_{INEL} = \frac{d\boldsymbol{\varepsilon}^{cr}}{d\tilde{\boldsymbol{\sigma}}}$$

$$\mathbf{S}_{INEL} = \begin{bmatrix} S_{11} & S_{12} & S_{13} & 2S_{14} & 2S_{15} & 2S_{16} \\ & S_{22} & S_{23} & 2S_{24} & 2S_{25} & 2S_{26} \\ & & S_{33} & 2S_{34} & 2S_{35} & 2S_{36} \\ & & & S_{44} & S_{45} & S_{46} \\ & & & & S_{55} & S_{56} \\ & & & & & S_{66} \end{bmatrix} \tag{7}$$

Notice the use of effective stress instead of applied stress. This is acceptable due to that fact the components of the applied stress terms within a component of effective stress are first order and thus terms of different indicial locations equate to zero upon differentiation. For components in the upper right symmetric zone (multiplied by two), such as $2S_{14}$, symmetry takes the following form, $2S_{14} = S_{41}$.

An input deck was coded in the ANSYS Parametric Design Language (APDL) and included all the commands necessary to perform a simulation. To establish the geometry, a single, three-dimensional, 8-noded block element was used. Constant force loading on the top four z-direction nodes was applied. Isothermal heating across the element was used. Appropriate displacement controls were set to allow deformation consistent with creep tests. The damage tensor, creep strain rate, and creep strain were initialized at zero. The elastic material properties E_p, E_z, ν_p, ν_{zp}, ν_{pz}, and G_{zp} were related to temperature-dependence in third order polynomial form.

Previous work by the authors using the isotropic Kachanov-Rabotnov model led to the development of creep material constants for GTD-111.[15] Since the anisotropic model reverts back to the isotropic model when γ is equal to zero, the earlier developed isotropic creep constants were used as initial values for the anisotropic model. The creep deformation response of the anisotropic model compared with the isotropic model is shown in Fig. 4. The model is shown to perform well with the given material. As shown in the figure, in the direction parallel to the uniaxial tensile load (loaded direction), the creep deformation remains the same between isotropic and the anisotropic model. Conversely, on directions perpendicular we see a reduction in the tertiary creep response of the material using the anisotropic model (when $\gamma = 1.0$ tertiary creep is completely removed leaving only secondary creep). This reduction is desired. Orientations where stress is not directly applied will not produce the same creep response as upon those where load is directly applied. The anisotropic model is thus a more accurate measure of the creep response of the material and will produce realistic and longer estimates of creep life. A limitation of the model is that the creep material constants are scalar and are based solely on the material orientation that interfaces with the uniaxial tensile load. The tertiary and secondary creep material constants remain the same and creep rate and damage evolution equations are simply scaled by γ and $\mathbf{n}_1$. A more robust method would include tensor based creep material constants where the local creep rate is conveyed through a global transformation tensor.

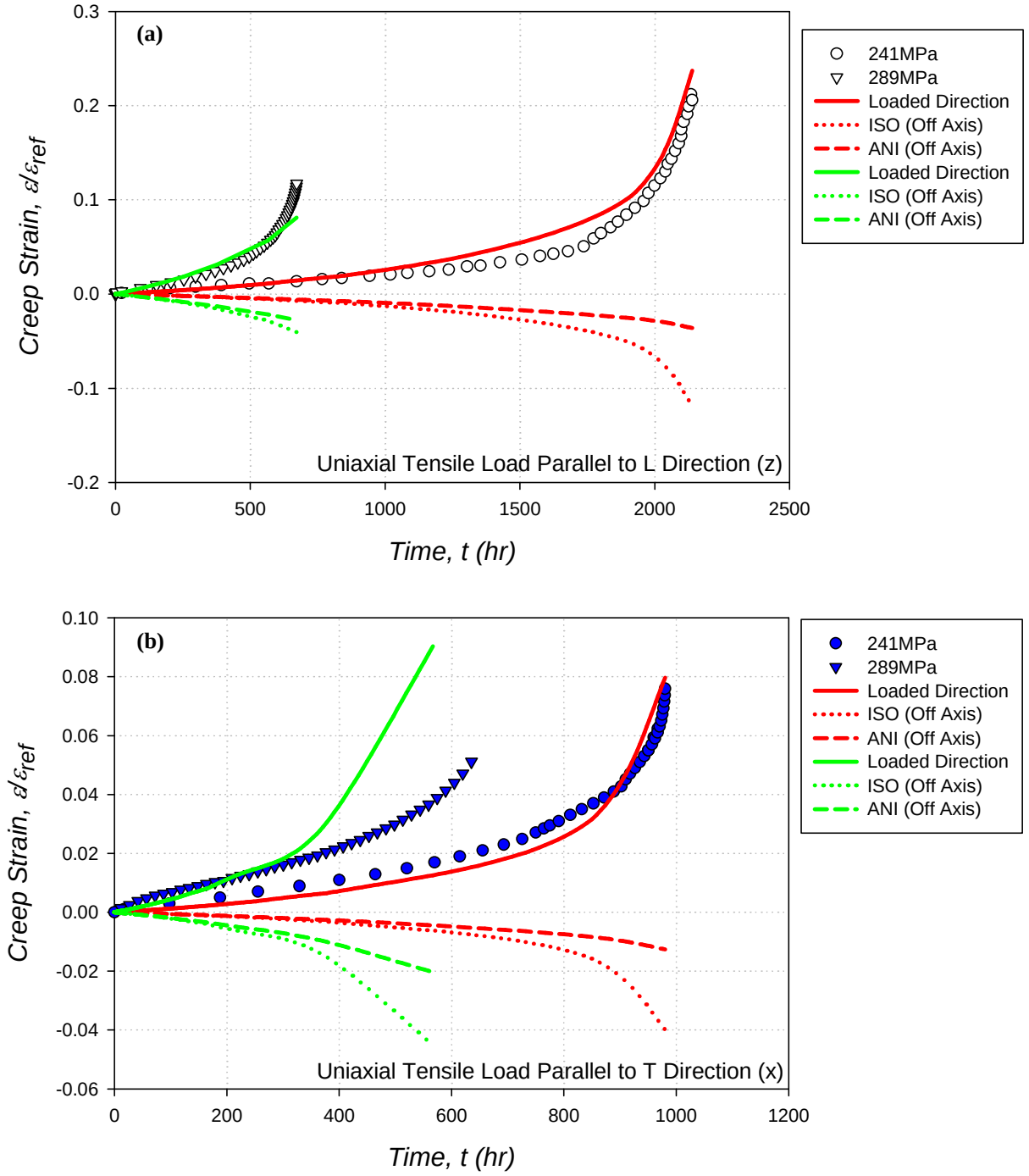

Figure 4. Comparison of experimental and FEM simulated creep deformation of GTD-111 @ 871°C (a) L-oriented: unfilled symbols (b) T-oriented: filled symbols

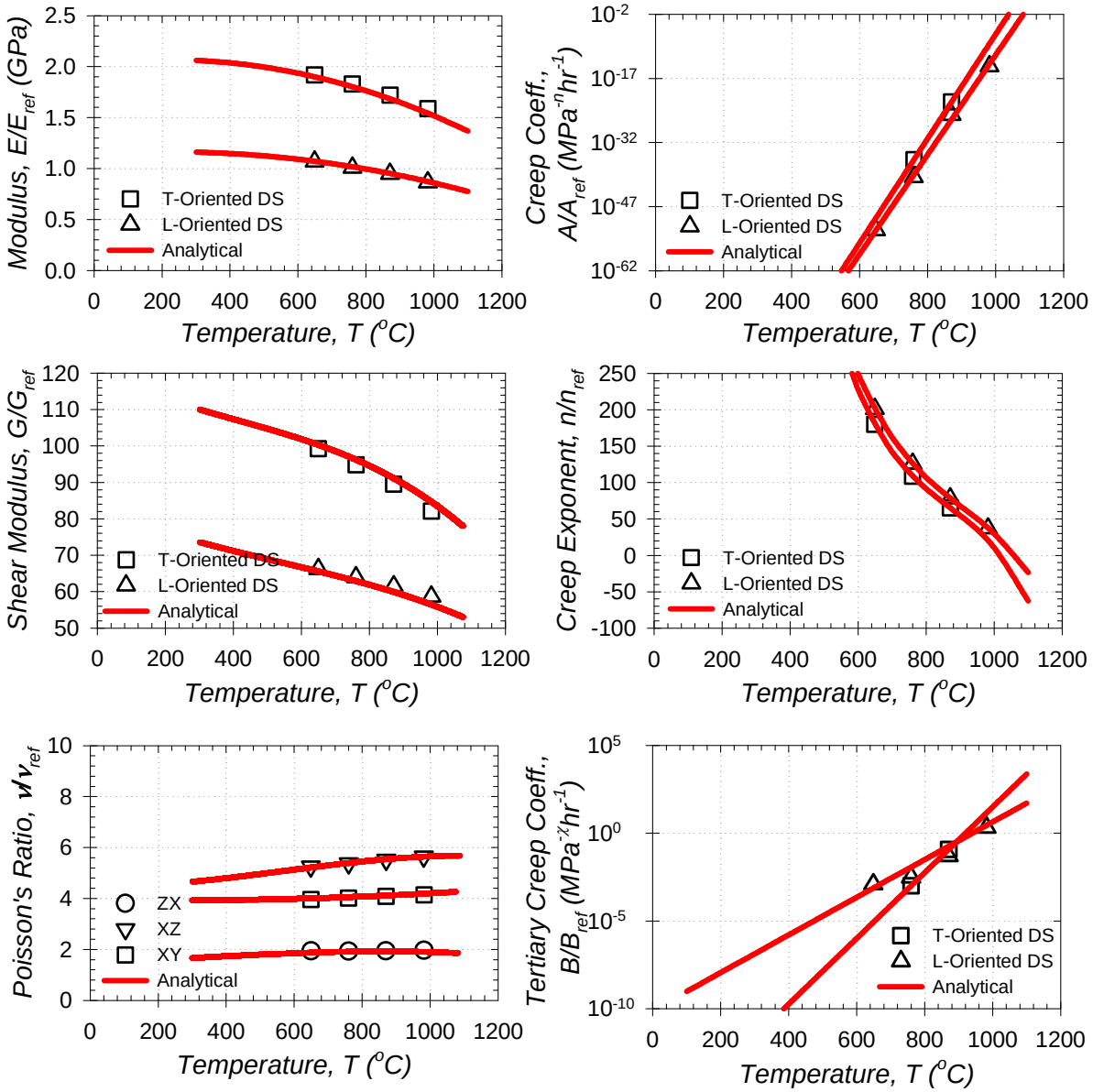

Figure 5. Plots of the temperature-dependence of elasticity and creep material constants

V. Temperature Dependence

All the creep curves can be generated through varying the creep constants, *A*, *n*, *B*, *l*, and *k*. After demonstrating that the anisotropic tertiary creep damage model can successfully model the creep deformation of GTD-111, constants were developed for temperatures range from 649 to 982°C. Regression analysis was utilized to determine temperature-dependence functions for each constant. The creep constants were considered stress-independent. The secondary creep constant, *A*, took on the standard Arrhenian temperature-dependent form, e.g.

$$A = A_0 \exp\left(\frac{Q_{cr}}{RT}\right) \quad . \tag{8}$$

where Q_{cr} is the apparent activation energy, A_0 is the temperature independent term, and T is temperature in Kelvin. R is the Boltzmann/universal gas constant. The secondary creep constant, n, was found to fit well as a third order polynomial, e.g.

$$n(T) = n_3 T^3 + n_2 T^2 + n_1 T^1 + n_0, \tag{9}$$

where T is measured in degrees Celsius. The tertiary creep constant B, was found to fit well as a secondary order exponential equation of the form, e.g.

$$B = B_1 \exp\left(B_0 T\right) \quad . \tag{10}$$

where B_0 and B_1 are constants and T is measured in degrees Celsius. The additional tertiary creep constants l and k were found to be temperature-independent. These temperature-dependent functions were created for both L-oriented and T-oriented creep tests using temperatures ranging from 649 and 982°C. The lowest square of the Pearson product-moment correlation coefficient, R^2, found within all the temperature-dependent functions was 0.94. The next lowest was 0.992. This demonstrates that using these functions the temperature-dependence of the model will closely mirror that of the creep deformation data.

VI. Orientation Dependence

As previously stated, GTD-111 is a transversely isotropic material. Both the elastic and creep response of this material depend on material orientation. To account for this phenomenon, the elasticity compliance tensor is used and orientation-dependent functions are needed to adjust the creep response. To that end, a creep test was performed at orientations of 45°, L (0°), and T (90°).

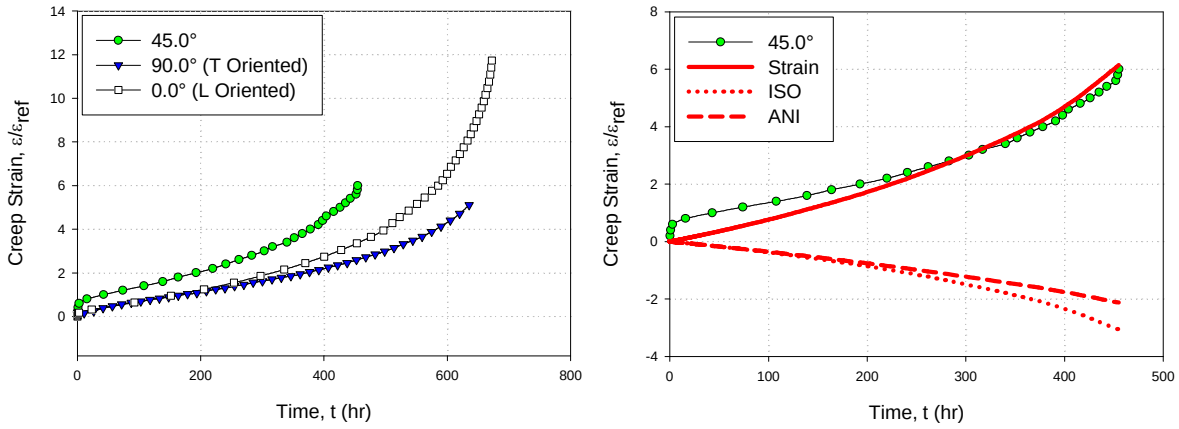

Figure 6. Creep deformation data with stress of 289MPa (a) L-T and 45° oriented specimen (b) comparison between experimental 45° oriented specimen and FEM simulated creep deformation

Figure 6a shows the resulting creep deformation. Since creep material constants for L & T-orientations are already known, numerical simulations of the 45° orientation was necessary. The fit of the numerical simulation is found in Fig. 6b, and shows that the constants replicate the experimental data well. Taking the creep constants for L, T, and 45° orientation-dependent constants were formulated. The secondary creep constant, A, was found to fit well in second order polynomial form, e.g.

$$A(\theta) = \left\langle A_2 \theta^2 + A_1 \theta^1 + A_0 \right\rangle + A_0, \tag{11}$$

where θ is measured in degrees. The McCauley brackets and the A_0 term are used to demonstrate that the minimum value of $A(\theta)$ can only be A_0. The secondary creep constant, n was found to fit well in the second order polynomial form, e.g.

$$n(\theta) = n_2 \theta^2 + n_1 \theta^1 + n_0, \tag{12}$$

where θ is measured in degrees. The tertiary creep constant, B, was found to best fit within a secondary order exponential equation of the form, e.g.

$$B(\theta) = B_1 \exp\left(B_0 \theta\right) \quad . \tag{13}$$

where B_0 and B_1 are constants and θ is measured in degrees. All together, regression analysis produced functions with a square of the Pearson product-moment correlation coefficient, R^2, of 0.9982 or greater. Figure 7 shows the fit of these orientation-dependent functions.

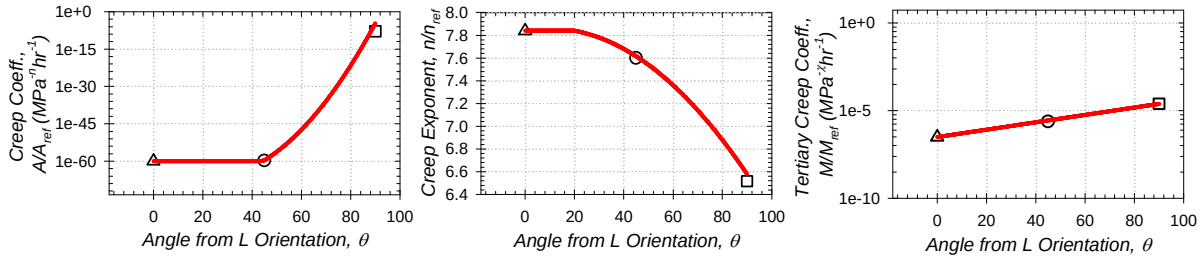

Figure 7. Creep material constants related to specimen orientation

Using the developed orientation-dependent functions, numerically the creep deformation of the model is parametrically exercised for various orientations. Figure 8 is the resulting creep deformation. It shows that the angle which produces the weakest creep resistance is between 45° and 90°. These orientations are weakest due to the ratio of textured and long grain boundaries. Literature has shown that grain boundary fluxes cause diffusion-induced grain-boundary migration and grain-boundary sliding activation.[16] The large volume fraction of long boundaries from the L-orientation coupled with the textural boundaries from the T-orientation influence the grain boundary state and subsequently, the stability of the material. This causes the creep resistance of GTD-111 at angles between 45° and 90° to be reduced. Further development of these orientation-dependent functions using additional creep tests at varying angles is necessary to verify that the numerically simulated deformation mirrors that of experiments.

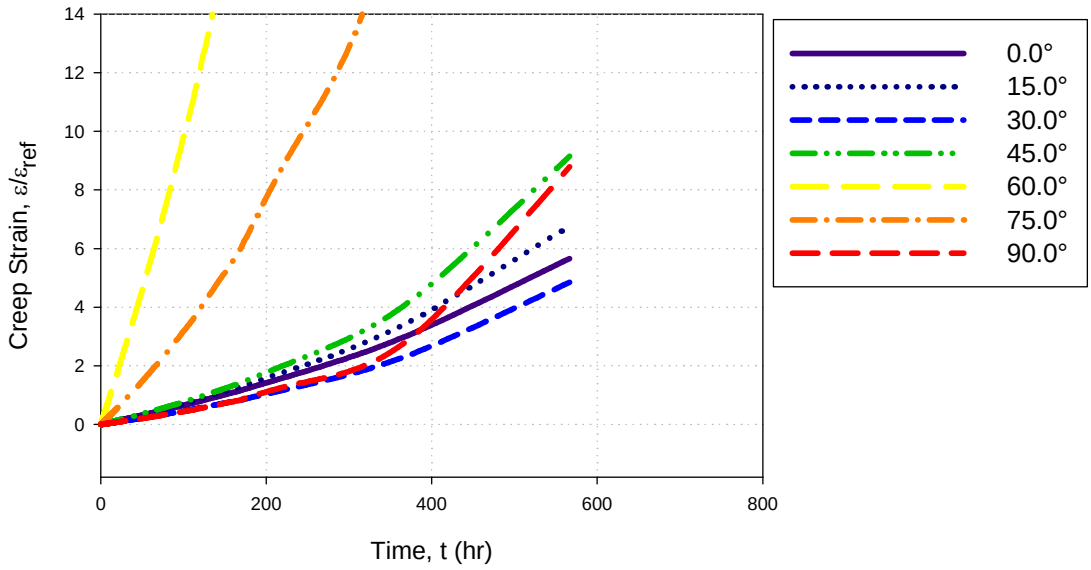

Figure 8. Numerically simulated creep deformation at 289MPa and 871°C for varies specimen orientations.

VII. Conclusion

The anisotropic tertiary creep damage model successfully models the experimental data for GTD-111 in L-oriented, T-oriented, and 45° specimen. It has been proven that the anisotropic model performance better than previous isotropic models due to the fact that it reduces the tertiary creep experienced by direction perpendicular to the uniaxial tensile load similar to what is observed experimentally.

Creep material constants were determined over a range of temperatures using creep deformation data from experimental creep tests. Using these constants, temperature-dependent functions were created. These functions allow the use of non-isothermal boundary conditions on components.

Taking the creep deformation data, constants were determined for the three orientations L-oriented, T-oriented, and 45°. Orientation-dependent functions were developed. This results in the model being able to adjust the creep response of a finite element dependent on the direction vector upon which stress load is applied.

Further development of this model can significantly enhance the ability of the aerospace and power generation industries to accurately predict the creep response of gas turbine components.

Acknowledgments

The authors would like to thank Richard W. Neu of Georgia Institute of Technology for 45°-oriented creep data. Calvin Stewart is thankful for the support of a McKnight Doctoral Fellowship through the Florida Education Fund.

References

[1]Daleo, J.A. and Wilson, J.R., "GTD111 alloy material study" *Journal of Engineering for Gas Turbines and Power*, Transactions of the ASME, Vol. 120, No. 2, 1998, pp. 375-382.

[2]Li, L., "Repair of directionally solidified superalloy GTD-111 by laser-engineered net shaping," *Journal of Materials Science*, Vol. 41, No. 23, 2006, pp. 7886-7893.

[3]Ibanez, A. R., Srinivasan, V. S., and Saxena, A., "Creep deformation and rupture behaviour of directionally solidified GTD 111 superalloy," *Fatigue & Fracture of Engineering Materials & Structures*, Vol. 29, No.12, 2006, pp. 1010 – 1020.

[4]Sajjadi, S. A., and Nategh, S., "A high temperature deformation mechanism map for the high performance Ni-base superalloy GTD-111," *Materials Science and Engineering A*, Vol. 307, No. 1-2, 2001, pp. 158-164.

[5]Hale, J. M., "Procedure development for the repair of GTD-111 gas turbine bucket material," *Eighth Congress &Exposition on Gas Turbines in Cogeneration and Utility*, Portland, OR, 1994.

[6]Stewart, C. M., and Gordon, A. P., "Modeling the Temperature-dependence of Tertiary Creep Damage of a Ni-Base Alloy," *ASME Early Career Technical Journal*, Vol. 7, No. 1, 2008, pp. 1-8.

[7]Murakami, S. and Sanomura, Y. "Creep and creep damage of copper under multiaxial states of stress," *In Plasticity Today*, edited by A. Sawczuk and G. Bianci, 1985, pp. 535–551.

[8]Altenbach H., Huang C., and Naumenko K., "Creep-damage predictions in thin-walled structures by use of isotropic and anisotropic damage models," *Journal of strain analysis for engineering design*, Vol. 37, No. 3, 2002, pp. 265-275.

[9]Kachanov, L. M., "Time to Rupture Process Under Creep Conditions," *Izv. Akad. Nank.*, Vol. 8, 1958, pp. 26-31.

[10]Rabotnov, Y. N., *Creep Problems in Structural Members*, North-Holland Publ. Co, North Holland, Amsterdam, 1969.

[11]Hayhurst, D. R., "On the Role of Continuum Damage on Structural Mechanics," *Engineering Approaches to High Temperature Design*, edited by B. Wilshire and D. R. Owen, Pineridge Press, Swansea, 1983, pp. 85-176.

[12]Murakami, S. "A continuum mechanics theory of anisotropic damage," *In Yielding, Damage and Failure of Anisotropic Solids*, edited by J. P. Boehler, Mechanical Engineering Publications, London, 1990, pp. 465–482.

[13]Murakami, S. and Ohno, N. "A continuum theory of creep and creep damage.," *In Creep in Structures*, edited by A. R. S. Ponter and D. R. Hayhurst, 1981, pp. 422–443.

[14]Hayhurst, D. R., "Creep Rupture Under Multi-Axial States Of Stress," *Journal of the Mechanics and Physics of Solids*, Vol. 20, No. 6, 1972, pp. 381-382.

[15]Gordon, A. P., Khan, S., and Nicholson D. W., "Temperature and Orientation Dependence of Creep Damage of Two Ni-Base Superalloys," *Proceedings of the 2007 ASME Pressure Vessels and Piping/CREEP8 Conference*, San Antonio, Texas, 2007.

[16]Kolobov, Yu.R., Grabovetskaya, G.P., Ivanov, K.V. and Ivanov, M.B., "Grain Boundary Diffusion and Mechanisms of Creep of Nanostructured Metals," *Interface Science*, Vol. 10, 2002, pp. 31–36.